


RESEARCH ARTICLE | APRIL 12 2018

# Wetting of water on graphene nanopowders of different thicknesses

Bijoyendra Bera; Noushine Shahidzadeh; Himanshu Mishra; Liubov A. Belyaeva; Grégory F. Schneider; Daniel Bonn 

 Check for updates

*Appl. Phys. Lett.* 112, 151606 (2018)

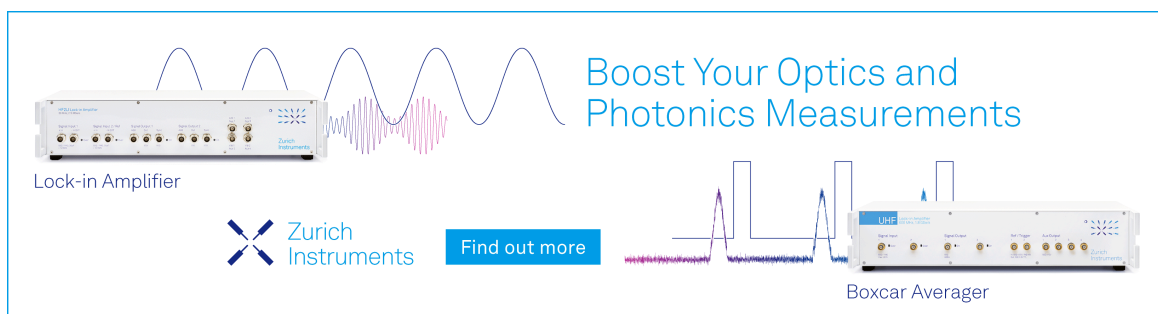
<https://doi.org/10.1063/1.5022570>



View Online




Export Citation



Boost Your Optics and Photonics Measurements

Lock-in Amplifier

 Zurich Instruments

[Find out more](#)

Boxcar Averager

## Wetting of water on graphene nanopowders of different thicknesses

Bijoyendra Bera,<sup>1,a)</sup> Noushine Shahidzadeh,<sup>1</sup> Himanshu Mishra,<sup>2</sup> Liubov A. Belyaeva,<sup>3</sup> Grégory F. Schneider,<sup>3</sup> and Daniel Bonn<sup>1</sup>

<sup>1</sup>*Soft Matter Group, Institute of Physics (IoP), Science Park 904, 1098 XH Amsterdam, The Netherlands*

<sup>2</sup>*King Abdullah University of Science and Technology (KAUST), Water Desalination and Reuse Center (WDR), Biological and Environmental Sciences and Engineering Division (BESE), Thuwal 23955-6900, Saudi Arabia*

<sup>3</sup>*Institute of Chemistry, Supramolecular & Biomaterials Chemistry, Leiden University, 2333 CC Leiden, The Netherlands*

(Received 16 January 2018; accepted 30 March 2018; published online 12 April 2018)

We study the wetting of graphene nanopowders by measuring the water adsorption in nanopowder flakes of different flake thicknesses. Chemical analysis shows that the graphene flakes, especially the thin ones, might exist in the partially oxidized state. We observe that the thinnest graphene nanopowder flakes do not adsorb water at all, independent of the relative humidity. Thicker flakes, on the other hand, do adsorb an increasing amount of water with increasing humidity. This allows us to assess their wetting behavior which is actually the result of the competition between the adhesive interactions of water and graphene and the cohesive interactions of water. Explicit calculation of these contributions from the van der Waals interactions confirms that the adhesive interactions between very thin flakes of graphene oxide and water are extremely weak, which makes the flakes superhydrophobic. “Liquid marble” tests with graphene nanopowder flakes confirm the superhydrophobicity. This shows that the origin of the much debated “wetting transparency” of graphene is due to the fact that a single graphene or graphene oxide layer does not contribute significantly to the adhesion between a wetting phase and the substrate. © 2018 Author(s). All article content, except where otherwise noted, is licensed under a Creative Commons Attribution (CC BY) license (<http://creativecommons.org/licenses/by/4.0/>).

<https://doi.org/10.1063/1.5022570>

Atomically thin layers of graphene exhibit an exceptionally rich range of mechanical and electronic properties such as high mechanical strength, chemical stability, optical transparency, and high electrical and thermal conductivities.<sup>1,2</sup> As a result, graphene has become one of the most active areas of scientific research in the last decade.<sup>3–5</sup> Among many others, potential applications of graphene in water desalination,<sup>6</sup> electrochemistry,<sup>7</sup> and catalysis<sup>8</sup> are being explored intensively. However, a clear understanding of the physical interactions between graphene and water has remained elusive. Recent experiments have shown that the contact angle of water on graphene-coated substrates and the contact angle of water on the same substrates without a graphene coating are almost identical, which suggests that graphene is wetting-transparent.<sup>9</sup>

The “wetting transparency” of graphene was first reported by Rafiee *et al.*<sup>9</sup> based on static contact angle measurements with water drops on graphene-coated *Si* and *Au* substrates. On *Si* and *Au*, the contact angle of a water drop is shown to be  $\sim 33^\circ$  and  $\sim 77^\circ$ , respectively, both with and without a graphene layer present on the substrate. Subsequently, a debate ensued regarding the nature of the interactions. Calculations of the van der Waals and short range repulsive forces suggest that a graphene layer would alter the wetting properties on superhydrophilic and superhydrophobic substrates.<sup>10</sup> Hence, wetting transparency of graphene will break down on such superhydrophilic or superhydrophobic substrates. Contact

angle measurements by Raj *et al.*,<sup>11</sup> on the other hand, demonstrated that contact angles are independent of the number of graphene layers on a glass or on a silicon oxide substrate. They also pointed out the influence of the substrate material on the wettability of graphene coated substrates. The possible role of contamination in such experiments has also been extensively discussed.<sup>12–14</sup>

To assess the wetting properties of water on graphene only, we use an entirely different experimental approach, involving only graphene flakes and no substrates: we measure the water adsorption from water vapor on graphene/graphene oxide nanoflakes of different thicknesses. In all the experiments and simulations reported in the literature, the wetting phase water is invariably introduced in the form of a sessile drop.<sup>15</sup> However, there is another way of assessing the wetting properties of a liquid on a given substrate,<sup>16</sup> namely, to measure the thickness of adsorbed water films from the vapor phase as the relative humidity (RH) is gradually increased. If the adhesive interactions are strong, a large amount of water will condense onto the substrate. The quantity of adsorbed water is given by the tradeoff between the energy cost of condensing water from an unsaturated vapor and the adhesive energy gain of having a water film at the surface.<sup>17</sup> In these water adsorption experiments with graphene nanopowder, the presence of a very large surface area also minimizes the effects of surface contamination. The flakes are of different thicknesses, and so, we can measure the adsorption properties as a function of the number of graphene layers without relying on a non-graphene solid substrate. In agreement with the

<sup>a)</sup>Electronic mail: b.bera@uva.nl

proposed wetting transparency, we find that for molecularly thin graphene or graphene oxide, the contact angle of water is indistinguishable from  $180^\circ$ . Our calculation of the adhesive van der Waals forces shows that a molecular layer is too thin to make a significant contribution, making also the difference between graphene and graphene oxide inconsequential while investigating graphene's wetting behavior.

Graphene nanopowders were obtained from Graphene Supermarket, NY, USA. We use three different flake thicknesses: 1.6 nm, 8 nm, and 50 nm. To characterize these graphene nanopowder flakes, we use Nova-Nano high resolution SEM, transmission electron microscopy (TEM), energy dispersive X-ray spectroscopy (EDS), and electron energy loss spectroscopy (EELS). For more details, see [supplementary material \(SI\)](#).

We can obtain the number of graphene layers ( $N$ ) present in the nanopowder sample from Raman spectroscopy data following the relation<sup>18</sup>  $\omega_G = 1581.6 + \frac{11}{(1+N)^{1.6}}$ , where  $\omega_G$  is the wavenumber corresponding to the G-peak. The calculation applied to our Raman spectra yields  $N \sim 1$ ,  $N \sim 4-5$ , and  $N \sim 25$ , respectively, for the three nanopowder samples. The graphene thickness is the same as that of  $p_z$  orbitals, while the interplane distance between two graphene layers in graphite<sup>3</sup> is  $\sim 0.3$  nm. Henceforth, we will refer to the different nanopowder samples with different thicknesses by indicating the number of layers ( $N$ ) calculated from the Raman spectra. The specific surface areas (measured by the Brunauer-Emmett-Teller or BET method by the supplier) of  $N \sim 1$ ,  $N \sim 4-5$ , and  $N \sim 25$  thick graphene nanopowder samples are  $500 \text{ m}^2/\text{g}$ ,  $100 \text{ m}^2/\text{g}$ , and  $20 \text{ m}^2/\text{g}$ , respectively. One key point is whether the nanopowder flakes are oxidized or not. Because the flakes are extremely thin, even if they are transported and handled under a nitrogen atmosphere and used in an ultraclean chamber, they are prone to be oxidized.<sup>19</sup> Raman spectroscopy shows that the thinnest flakes are partially oxidized. The peaks in the Raman spectra are reminiscent of graphene oxide (GO) or reduced graphene oxide (r-GO).<sup>20,21</sup> The thicker flakes, 8 nm and 50 nm thick, are less prone to getting oxidized because of their smaller surface-to-volume ratio. Figure 1 shows typical Raman spectra peaks of few layer graphene or reduced graphene oxide. 1.6 nm thick flakes show Raman features typical for GO and r-GO, while 8 nm and 50 nm thick flakes have Raman

features typical for a few-layer graphene or r-GO,  $I_D/I_G$  ratio around 0.1 and  $I_{2D}/I_G$  ratio around 0.3, indicating higher crystallinity and lower defect density.

The water adsorption experiments are performed using a precision mass balance with a precision of  $10^{-4}$  g in a protected environment (nitrogen atmosphere) of a climatic chamber in order to control the relative humidity (RH). The nanopowder is placed on an open polystyrene or glass petridish (of diameter 5.5 cm) taking precautions so that the outside relative humidity (RH) and contaminants do not affect the sample (Fig. S5, [supplementary material](#)). We keep the surface areas of the samples [i.e., specific surface area (BET)  $\times$  initial mass ( $m_0$ )] constant in the experiments. The mass of each sample is recorded every 10 minutes during the experiment. The RH is fixed by controlling  $p_w$ , the partial water vapor pressure. A water bath thermostat is used to let nitrogen flow through water at a temperature  $T_1$  and flows into the climatic chamber at  $T_2 = 21^\circ\text{C}$ . Hence, partial vapor pressure at temperature  $T_2$  equals the saturated vapor pressure at temperature  $T_1$ , and the RH is as follows:  $\text{RH} = \frac{p_{ws}(T_1)}{p_{ws}(T_2)} \cdot 100\%$ .<sup>22</sup> RH was changed from 5% to 95% in steps of 10%. We wait typically for 3 h at each RH step for the mass to reach an equilibrium value.

Figure 2 shows the mass of water  $m$  adsorbed by the flakes when the relative humidity (RH) is changed. The layer of nanopowder with the thinnest flake size ( $N \sim 1$ ) does not adsorb any water even at the highest RH. In contrast, the nanopowder consisting of 4–5 layers of graphene adsorbs a considerable amount of water and the 25 layer thick flakes even more. Knowing the specific surface area  $a$  (the BET), we can deduce the thickness of the adsorbed film  $h = \frac{m}{m_0 a \rho}$ , with  $\rho$  being the density of water (Fig. 2). As mentioned already, the electron microscopy (in [supplementary material](#)) and Raman spectra data show that we do not probe pristine graphene layers in these experiments. The flakes have quite a lot of edges, kinks, and bends. However, as long as the surface area of the sample is significantly smaller than that of the edges and kinks, one can still reliably perform the water sorption experiments. With a density of  $\sim 2 \text{ g}/\text{cm}^3$  and a typical flake size of  $10 \mu\text{m} \times 10 \mu\text{m} \times 1 \text{ nm}$  (the details are given in the [supplementary material](#)), one can calculate how many water molecules constitute a monolayer on the surface and on the edges. Taking  $2 \text{ \AA} \times 2 \text{ \AA}$  as the typical size of an

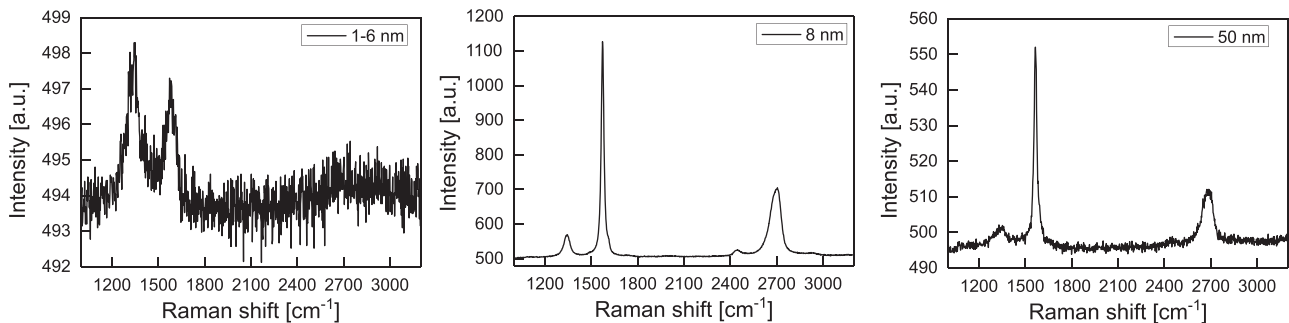


FIG. 1. **Raman spectroscopy on graphene nanoflakes.** The relative thickness of these samples provided by the manufacturer (1:5:31) agrees rather well with our number of graphene layers calculated from Raman data (1:5:25). The samples with a flake size of 1.6 nm show Raman features typical for GO and r-GO,  $I_D/I_G$  ratio close to 1 and wide and low-intensity 2D bands, indicating high defect density and partial lattice disordering due to oxidized edges. Samples with 8 nm and 50 nm flake sizes have Raman features typical for a few-layer graphene or r-GO,  $I_D/I_G$  ratio around 0.1 and  $I_{2D}/I_G$  ratio around 0.3, indicating higher crystallinity and lower defect density.

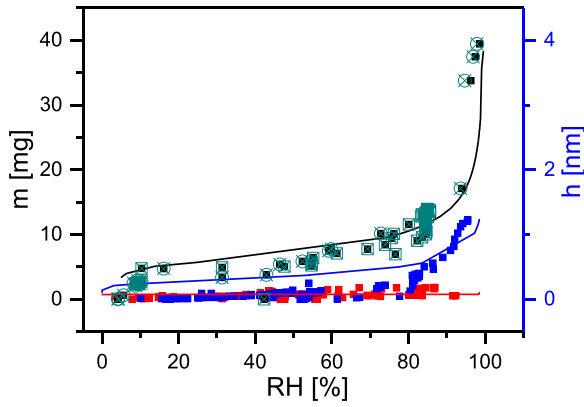


FIG. 2. Adsorbed water and water film thickness as a function of relative humidity for graphene nanopowder of various flake thicknesses. The square symbols signify separate sets of experiments where one datapoint in each set is an average of 10 independent experiments under the same conditions. Continuous lines depict the predicted moisture adsorption for graphene nanopowders: 1 layer (red), 4–5 layers (blue), and 25 layers (black). In addition, the adsorbed film thickness  $h$  in the case of 50 nm thick graphene nanopowder is also shown with the crossed open symbols.

adsorbed water molecule, one finds  $\approx 10^{22}$  molecules on the surface and  $\approx 2 \cdot 10^{18}$  molecules on the edges. Hence, the edge effects are negligible since they are 4 orders of magnitude smaller. Finally, adsorption of water above a certain RH can imply capillary condensation which is multilayer adsorption from the vapor phase into the porous medium below the saturation vapor pressure of the pure liquid. However, water sorption is reversible in our experiments and shows no hysteresis. We verified that the moisture adsorption trends show no hysteresis by comparing the results for increasing RH (from 5% to 90%) with the results for decreasing RH (from 90% to 5%); this excludes capillary condensation between the graphene nanopowder flakes<sup>16,17</sup> or at kinks and defects in the graphene.

To understand the mass adsorption characteristics, we start with the reasonable assumption that the adhesive interaction between the water and the flakes is due to the van der Waals forces. These can be calculated and compared with our adsorption experiments. Our system consists of a few molecular layer thick graphene [Fig. 3(a)]; in this case, the adhesion force per unit area can be written as<sup>23</sup>

$$\Pi_{vdw}(h) = -\frac{1}{6\pi} \frac{A_{132}}{h^3} - \frac{1}{6\pi} \frac{A_{12/31}}{(h+t)^3}, \quad (1)$$

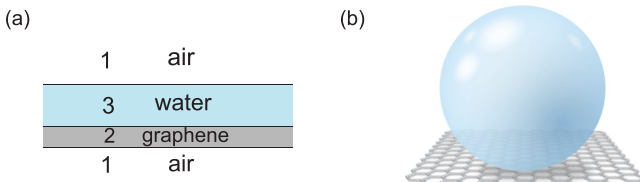


FIG. 3. Connecting graphene wettability to fundamentals of adhesion through van der Waals Interactions. (a) Schematic of graphene wetting represented as an adsorbed water film of thickness  $h$ . (b) Schematic of graphene's wetting transparency in air: the van der Waals interactions between graphene and water molecules are so much smaller than those between the water molecules themselves that the equilibrium contact angle is  $\approx 180^\circ$ .

where  $A_{132}$  is the Hamaker constant with interactions between the interfaces 12 (air-graphene) and 32 (water-graphene) in consideration,  $A_{12/31}$  is that between 12 (air-graphene) and 31 (air-water),  $t$  is the flake thickness, and  $h$  is the adsorbed water film thickness. The equilibrium film thickness  $h_{eq}$  follows from the equilibrium between the adhesion forces and the free energy cost of condensing the water from the unsaturated vapor.<sup>16,23</sup> It follows that

$$\Pi(h_{eq}) = \Pi_{vdw} + \frac{\Delta\mu}{v_{w,molar}} = 0, \quad (2)$$

where  $\Delta\mu = RT \ln\left(\frac{p}{p_{sat}}\right) = RT \ln\left(\frac{RH}{100}\right)$  is the chemical potential difference between the experimental and saturated relative humidity and  $v_{w,molar}$  is the molar volume of water at room temperature.

The Hamaker constant  $A_{12/31}$  can be calculated by noting that  $A_{12/31} = \sqrt{A_{121}A_{313}}$ . Using Lifshitz theory of van der Waals forces with Derjaguin approximation (DLP) theory,<sup>23</sup> we have calculated the Hamaker constants from the known refractive indices and the dielectric constants. The details of the calculation are provided in the [supplementary material](#). Eqs. (1) and (2) can then be solved for  $\Delta\mu$ , and the calculated trend of adsorbed mass as a function of RH agrees quite well with the experiments (Fig. 2) without any adjustable parameters. The slight overestimation, in the theory, of the water film thickness for low RH is likely to be due to the fact that the calculation of the Hamaker constants is not straightforward since one of our phases is water which has a high dielectric constant and many optical absorption bands.<sup>24</sup>

These results show that for the molecularly thin graphene oxide/reduced graphene oxide ( $N=1$ ), the mass of adsorbed water and hence the equilibrium film thickness are indistinguishable from zero, even *at* coexistence, i.e., at 100% relative humidity. In agreement with the experimental and calculated water adsorption data, the van der Waals adhesive interactions between a water drop and a single graphene layer are extremely weak, leading to a contact angle of  $\sim 180^\circ$ . The contact angle  $\theta$  of the drop in the solid phase can be calculated directly from the disjoining pressure  $\Pi(h)$ ; the spreading parameter  $S$  can be written as

$$S = \int_{h_{eq}}^{\infty} \Pi(h) dh, \quad (3)$$

i.e., by calculating the work necessary against the van der Waals forces to go from a film of thickness  $h_{eq}$  to an infinitely thick film.<sup>25</sup> Young's equation then gives the contact angle as

$$\cos \theta = 1 + \frac{S}{\gamma_{lv}}. \quad (4)$$

The calculation then leads to  $\theta = 179.3^\circ$ ,  $163.2^\circ$ , and  $139.7^\circ$  ( $\pm 2^\circ$ ) for the three graphene flake thicknesses of  $N \sim 1$ ,  $N \sim 4-5$ , and  $N \sim 25$ , respectively. This shows that the thinnest flakes of graphene oxide ( $N \sim 1$ ) are indeed superhydrophobic.

An independent test of the observation that the contact angle of water on the thinnest graphene nanopowder flake is indistinguishable from  $180^\circ$  can be obtained by attempting

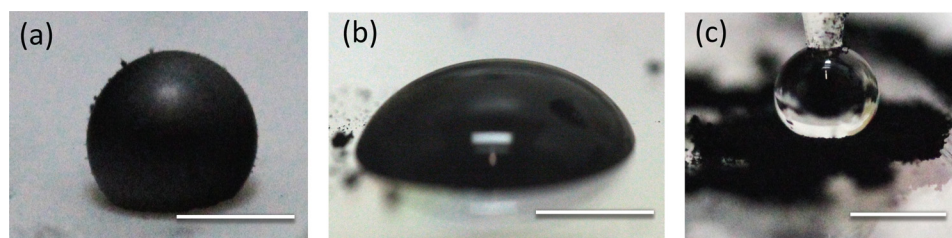


FIG. 4. Graphene powders of different flake thicknesses in contact with a water drop; (a) 4–5 layer graphene, (b) 25 layer graphene, and (c) 1 layer graphene. The scale bars in (a), (b), and (c) represent a length of 2 mm. In (a), there is graphene on the liquid vapor interface, in (b), there is graphene in the suspension but not at the droplet surface, and in (c), there is no graphene on the surface of the water droplet.

to adsorb the flakes onto a water drop. If adhesive interaction is present, the flakes will adhere to the liquid drop, coating the whole surface in the process. This phenomenon is well known for hydrophobic particles adsorbing onto water drops, leading to the formation of “liquid marbles,” or pearls, which are liquid drops encapsulated by a hydrophobic powder. This results in a powder-coated drop that rolls very easily over any solid substrate, and in the past, the properties of such drops have been investigated in detail.<sup>26,27</sup> Theoretically, it has been firmly established that particles of a material with a contact angle smaller than  $180^\circ$  should adsorb onto the surface of a liquid drop to form such liquid marbles since the system gains the adhesion energy between the powder and the drop.<sup>28</sup>

In our “liquid graphene marble” experiments, the different graphene nanopowders are placed onto flat polystyrene substrates. Putting a water droplet (volume  $5\ \mu\text{l}$ ) onto the powder indeed leads to the spontaneous formation of a liquid marble for the intermediate thickness (4–5 layers) flakes [Fig. 4(a)]. As expected, the resulting drop has a very large contact angle and rolls easily over the surface. For the thickest flakes (25 layers), the powder covers the surface but a small part of the powder even intrudes into the water, implying that the powder is no longer sufficiently hydrophobic to form perfect marbles, and a drop with a finite contact angle ensues, with the graphene being inside the drop rather than at its surface [Fig. 4(b)]. In contrast, the molecularly thin flakes are not even adsorbed onto the surface, implying that there is no measurable adhesive interaction between the graphene and the water even when the graphene exists in an oxide or a reduced oxide form [Fig. 4(c)]. All these observations are in line with the mass measurements above and confirm that the contact angle of water on molecularly thin reduced graphene oxide flakes is  $\sim 180^\circ$ .

These findings rationalize previous observations on the wetting properties and wetting transparency of graphene. It follows that if the graphene is fixed on a substrate, the latter contributes significantly to the adhesive interactions with the water drop, in agreement with the reported observations<sup>9</sup> of the wetting transparency of graphene. Our results are independent of a specific substrate. We treat graphene nanopowder as a porous medium, where the amount of water adsorbed follows a BET type of adsorption isotherm and thus only depends on the flake thickness. Our method allows us to avoid the issues of contamination and corrugation of the graphene-substrate interface.<sup>14</sup> Instead of performing contact angle measurements, the wetting transparency of our thinnest flakes is shown through the adsorption experiments

and is further supported by the calculation of van der Waals type of interaction in the system. These thinnest flakes are not pristine graphene but rather graphene oxide or reduced graphene oxide. However, this is inconsequential for the arguments here; the main point is that in a single molecular layer, there are not enough molecules to create significant adhesion (due to the van der Waals forces) with water; this holds for both graphene and molecularly thin graphene oxide. If the substrate is air and graphene is wetting transparent, the contact angle is  $180^\circ$  since the contact angle of a water drop in air is  $180^\circ$ . This is what we find. If the substrate is different, the van der Waals interaction of the liquid with the substrate is dominant over the graphene contribution, simply because the number of graphene atoms scales with the system size squared (2 dimensions), whereas the number of substrate atoms scales with the system size cubed (3 dimensions). It is for this reason that graphene is wetting transparent. The contact angle is always a tradeoff between the cohesion of liquid molecules in the drop, which favors an angle of  $180^\circ$  (because a sphere has the largest volume to surface ratio), and the adhesion of the liquid on the surface which favors a smaller contact angle to enlarge the adhesive contact area. The adhesion is larger for thicker graphene since more carbon atoms contribute to the adhesive interaction with the surface.

See [supplementary material](#) for the details of characterization of graphene nanopowder samples (using electron microscopy and X-ray spectroscopy), the water adsorption experimental set-up, and the calculation of the Hamaker constant and the corresponding adsorbed film thickness on graphene nanopowder flakes.

<sup>1</sup>C. Gomez-Navarro, J. C. Meyer, R. S. Sundaram, A. Chuvilin, S. Kurasch, M. Burghard, K. Kern, and U. Kaiser, “Atomic structure of reduced graphene oxide,” *Nano Lett.* **10**, 1144–1148 (2010).

<sup>2</sup>C.-J. Shih, M. S. Strano, and D. Blankschtein, “Wetting translucency of graphene,” *Nat. Mater.* **12**, 866–869 (2013).

<sup>3</sup>K. S. Novoselov, A. K. Geim, S. V. Morozov, D. Jiang, Y. Zhang, S. V. Dubonos, I. V. Grigorieva, and A. A. Firsov, “Electric field effect in atomically thin carbon films,” *Science* **306**, 666–669 (2004).

<sup>4</sup>A. K. Geim, “Graphene: Status and prospects,” *Science* **324**, 1530–1534 (2009).

<sup>5</sup>A. K. Geim and K. S. Novoselov, “The rise of graphene,” *Nat. Mater.* **6**, 183–191 (2007).

<sup>6</sup>A. H. Castro Neto, F. Guinea, N. M. R. Peres, K. S. Novoselov, and A. K. Geim, “The electronic properties of graphene,” *Rev. Mod. Phys.* **81**, 109–162 (2009).

<sup>7</sup>M. S. Dresselhaus, “Fifty years in studying carbon-based materials,” *Phys. Scr.* **T146**, 014002 (2012).

<sup>8</sup>C. Oshima and A. Nagashima, “Ultra-thin epitaxial films of graphite and hexagonal boron nitride on solid surfaces,” *J. Phys.: Condens. Matter* **9**, 1 (1997).

- <sup>9</sup>J. Rafiee, X. Mi, H. Gullapalli, A. V. Thomas, F. Yavari, Y. Shi, P. M. Ajayan, and N. A. Koratkar, "Wetting transparency of graphene," *Nat. Mater.* **11**, 217–222 (2012).
- <sup>10</sup>C.-J. Shih, Q. H. Wang, S. Lin, K.-C. Park, Z. Jin, M. S. Strano, and D. Blankschtein, "Breakdown in the wetting transparency of graphene," *Phys. Rev. Lett.* **109**, 176101 (2012).
- <sup>11</sup>R. Raj, S. C. Maroo, and E. N. Wang, "Wettability of graphene," *Nano Lett.* **13**, 1509–1515 (2013).
- <sup>12</sup>Z. Li, Y. Wang, A. Kozbial, G. Shenoy, F. Zhou, R. McGinley, P. Ireland, B. Morganstein, A. Kunkel, S. P. Surwade, L. Li, and H. Liu, "Effect of airborne contaminants on the wettability of supported graphene and graphite," *Nat. Mater.* **12**, 925–931 (2013).
- <sup>13</sup>K. Xu and J. R. Heath, "Wetting: Contact with what?," *Nat. Mater.* **12**, 872–873 (2013).
- <sup>14</sup>L. A. Belyaeva, P. M. G. van Deursen, K. I. Barbetsea, and G. F. Schneider, "Hydrophilicity of graphene in water through transparency to polar and dispersive interactions," *Adv. Mater.* **30**, 1703274 (2017).
- <sup>15</sup>T. Ondarcuhu, V. Thomas, M. Nunez, E. Dujardin, A. Rahman, C. T. Black, and A. Checco, "Wettability of partially suspended graphene," *Sci. Rep.* **6**, 24237 (2016).
- <sup>16</sup>D. Bonn, J. Eggers, J. Indekeu, J. Meunier, and E. Rolley, "Wetting and spreading," *Rev. Mod. Phys.* **81**, 739–805 (2009).
- <sup>17</sup>D. Bonn and D. Ross, "Wetting transitions," *Rep. Prog. Phys.* **64**, 1085 (2001).
- <sup>18</sup>H. Wang, Y. Wang, X. Cao, M. Feng, and G. Lan, "Vibrational properties of graphene and graphene layers," *J. Raman Spectrosc.* **40**, 1791–1796 (2009).
- <sup>19</sup>L. Liu, S. Ryu, M. R. Tomasik, E. Stolyarova, N. Jung, M. S. Hybertsen, M. L. Steigerwald, L. E. Brus, and G. W. Flynn, "Graphene oxidation: Thickness-dependent etching and strong chemical doping," *Nano Lett.* **8**, 1965–1970 (2008).
- <sup>20</sup>S. Pei and H.-M. Cheng, "The reduction of graphene oxide," *Carbon* **50**, 3210–3228 (2012).
- <sup>21</sup>S. Abdolhosseinzadeh, H. Asgharzadeh, and H. Seop Kim, "Fast and fully-scalable synthesis of reduced graphene oxide," *Sci. Rep.* **5**, 10160 (2015).
- <sup>22</sup>J. Desarnaud, D. Bonn, and N. Shahidzadeh, "The pressure induced by salt crystallization in confinement," *Sci. Rep.* **6**, 30856 (2016).
- <sup>23</sup>J. Israelachvili, *Intermolecular and Surface Forces*, Revised 3rd ed. (Elsevier Science, 2011).
- <sup>24</sup>D. Bonn, E. Bertrand, N. Shahidzadeh, K. Ragil, H. T. Dobbs, A. I. Posazhennikova, D. Broseta, J. Meunier, and J. O. Indekeu, "Complex wetting phenomena in liquid mixtures: Frustrated-complete wetting and competing intermolecular forces," *J. Phys.: Condens. Matter* **13**, 4903 (2001).
- <sup>25</sup>E. Bertrand, H. Dobbs, D. Broseta, J. Indekeu, D. Bonn, and J. Meunier, "First-order and critical wetting of alkanes on water," *Phys. Rev. Lett.* **85**, 1282–1285 (2000).
- <sup>26</sup>P. Aussillous and D. Quere, "Liquid marbles," *Nature* **411**, 924–927 (2001).
- <sup>27</sup>T. Supakar, M. Moradiafrapoli, G. F. Christopher, and J. O. Marston, "Spreading, encapsulation and transition to arrested shapes during drop impact onto hydrophobic powders," *J. Colloid Interface Sci.* **468**, 10–20 (2016).
- <sup>28</sup>G. McHale and M. I. Newton, "Liquid marbles: Topical context within soft matter and recent progress," *Soft Matter* **11**, 2530–2546 (2015).